

## Supporting Information

### **A Nonflammable Electrolyte for Ultrahigh-Voltage (4.8 V-Class) Li||NCM811 Cells with A Wide Temperature Range of 100 °C**

*Peitao Xiao*<sup>1,2</sup>, *Yun Zhao*<sup>3</sup>, *Zhihong Piao*<sup>1</sup>, *Baohua Li*<sup>3</sup>, *Guangmin Zhou*<sup>1\*</sup>, and *Hui-Ming Cheng*<sup>1,4,5\*</sup>

<sup>1</sup> Shenzhen Geim Graphene Center, Tsinghua-Berkeley Shenzhen Institute & Tsinghua, Shenzhen International Graduate School, Tsinghua University, Shenzhen 518055, P. R. China

<sup>2</sup> College of Aerospace Science and Engineering, National University of Defense Technology, Changsha 410073, China

<sup>3</sup> Shenzhen Key Laboratory on Power Battery Safety and Shenzhen Geim Graphene Center, Tsinghua Shenzhen International Graduate School (SIGS), Shenzhen 518055, China

<sup>4</sup> Institute of Technology for Carbon Neutrality, Shenzhen Institute of Advanced Technology, Chinese Academy of Sciences, Shenzhen 518055, P. R. China

<sup>5</sup> Shenyang National Laboratory for Materials Science, Institute of Metal Research, Chinese Academy of Sciences, Shenyang 110016, China

#### AUTHOR INFORMATION

##### **Corresponding Authors**

\* [guangminzhou@sz.tsinghua.edu.cn](mailto:guangminzhou@sz.tsinghua.edu.cn);

\* [hmcheng@sz.tsinghua.edu.cn](mailto:hmcheng@sz.tsinghua.edu.cn)

## Methods

**Materials:** Bis(2,2,2-trifluoroethyl) carbonate (BTC) and 3Å molecular sieves were purchased from Aladdin. Fluoroethylene carbonate (FEC), ethylene carbonate (EC), diethyl carbonate (DEC), lithium hexafluorophosphate (LiPF<sub>6</sub>), and the commercial EC-based electrolyte were purchased from Dodo Chem. All the solvents were used after removing their water contents using 3Å molecular sieves for 3 days. The commercial electrolyte composed of 1 M LiPF<sub>6</sub> in EC:DEC (1:1 by volume) was used as the base electrolyte. 1M LiPF<sub>6</sub> was dissolved in FEC:BTC (3:7 by volume) to obtain the HV electrolyte.

**Electrochemical tests:** All the cells with different electrolytes were assembled in a glovebox using 2032-type coin cells with Celgard 2400 as separator and lithium metal as anode. The cathodes in Li||Cu, Li||Li, and Li||NCM811 were copper (Cu), lithium metal (450 μm), and LiNi<sub>0.8</sub>Co<sub>0.1</sub>Mn<sub>0.1</sub>O<sub>2</sub> (NCM811), respectively. NCM811 cathodes with mass loadings of 8~8.5 mg cm<sup>-2</sup> were supplied by Guangdong Canrd New Energy Technology Co.,Ltd. The theoretical capacity of NCM811 is about 1.7 mAh cm<sup>-2</sup>. In the Li||NCM811 full cells, thin lithium metal with a thickness of 50 μm was used as the anode. For the other cells, lithium metal with a thickness of 450 μm was used. The amount of electrolyte in each cell was about 30 ul. The diameters of cathode and anode electrodes are 14.5 and 15.6 mm, respectively.

Galvanostatic tests were conducted on a battery testing system (LAND, Wuhan China). Li-Cu cells were first cycled from 0-1 V at a current density of 0.05 mA to form the SEI and remove the contaminants on the Cu. Electrochemical impedance spectroscopy (EIS) was tested on a CHI 760D electrochemical workstation in the frequency range from 100 kHz to 0.01 Hz. This workstation was also used to record cyclic voltammetry (CV), linear sweep voltammetry (LSV), and constant voltage floating tests.

**Characterization:** A KRUSS DSA30 contact angle tester was used to measure the contact angles of different electrolytes on the separators. PHI 5000 VersaProbe II in-situ X-ray photoelectron spectroscopy (XPS) was used to analyze the SEI and CEI films. Ar ions were used to sputter for in-depth XPS tests. All binding-energy values were referenced to the C 1s peak of carbon at 284.8 eV. All samples were washed using EMC three times and dried in a glovebox before analysis. X-ray diffraction

(XRD) measurements were made on a D8 Advance X-ray diffractometer in the range of 10–70° at 0.5° min<sup>-1</sup>. A HITACHI SU8010 scanning electron microscopy (SEM) was used to examine the morphology of the deposited lithium. <sup>7</sup>Li nuclear magnetic resonance (NMR) spectra were obtained on a BRUKER AVANCEIIIHD 500 Nuclear Magnetic Resonance spectrometer. Structural characterization of the CEI was carried out on high resolution transmission electron microscopy (HRTEM, FEI Tecnai G2 spirit). ICP-MS (NexION 300X) was adopted to test the transition metal ions dissolution in different electrolytes. X-ray absorption near edge structure spectra were obtained at 1W1B station in Beijing Synchrotron Radiation Facility.

**Computational Details:** HOMO and LUMO energy levels of EC, DEC, FEC, BTC, and LiPF<sub>6</sub> were calculated using a Gaussian 09 software package with 6-311+ g (d, p) as the basis set. Li<sup>+</sup>-solvent binding energies were calculated from the following equation:

$$E_b = E_{Li^+ - S} - E_s - E_{Li^+}$$

where  $E_b$  is the binding energy between Li<sup>+</sup> and the different solvents,  $E_{Li^+ - S}$  is the total Gibbs energy of the Li<sup>+</sup>-solvent system,  $E_s$  and  $E_{Li^+}$  are the Gibbs energies of the solvents and Li<sup>+</sup>, respectively.

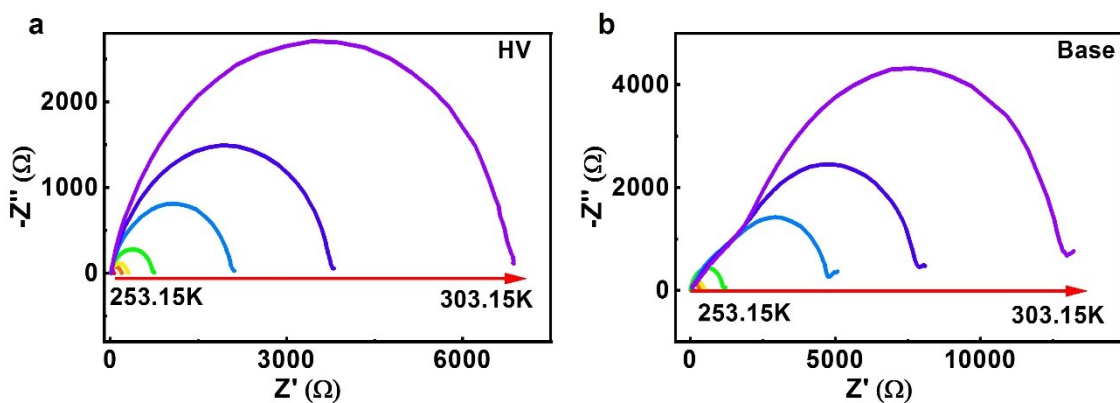


**Figure S1.** Nyquist plots of the EIS of Li||Li symmetric cells using (a) HV and (b) base electrolytes at different temperatures.

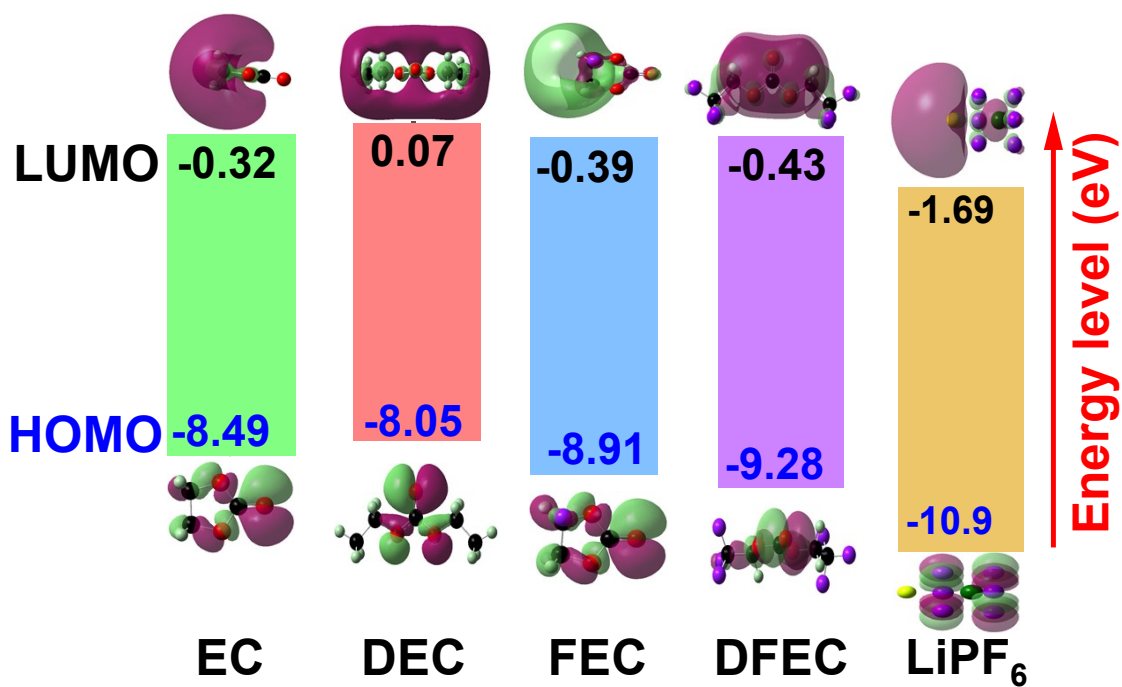


**Figure S2.** LUMO/HOMO energy levels of the solvents and lithium salt in the electrolytes.

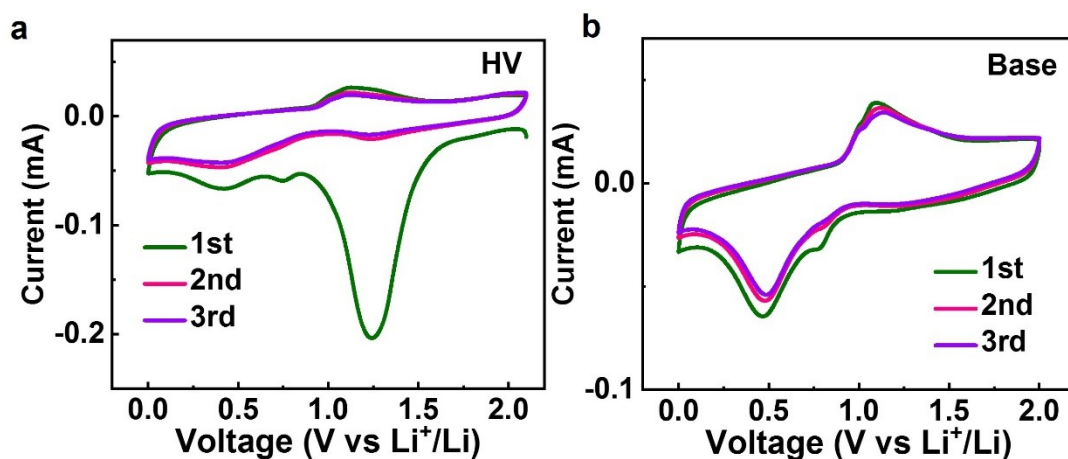


**Figure S3.** CV curves for 3 cycles at  $1 \text{ mV s}^{-1}$  for (a) HV and (b) base electrolytes.

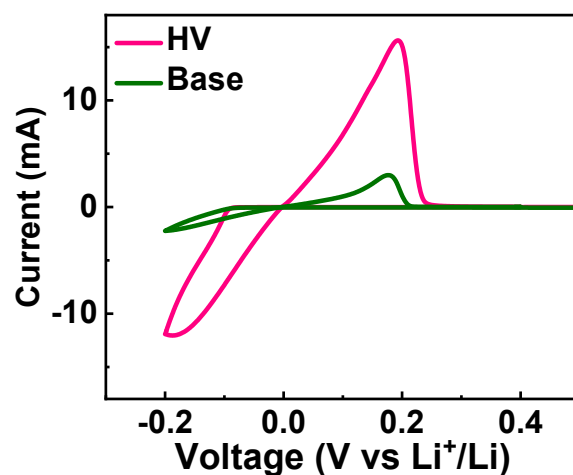


**Figure S4.** (a) CV curves of Li||Cu cells using the different electrolytes in the range  $-0.2 - 0.5 \text{ V}$  at  $1 \text{ mV s}^{-1}$ .

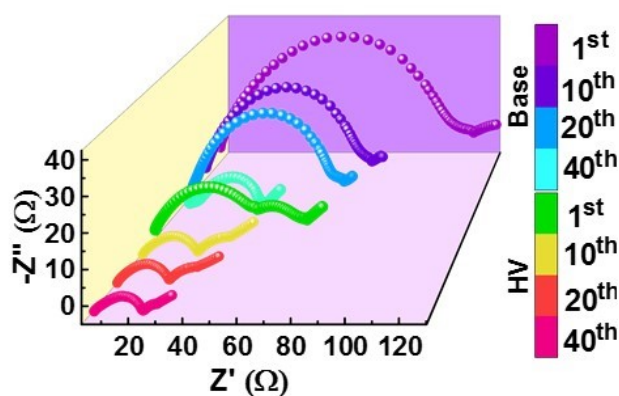


**Figure S5.** Nyquist plots of EIS for Li||Li symmetrical cells in HV and base electrolytes before and after different numbers of cycles.

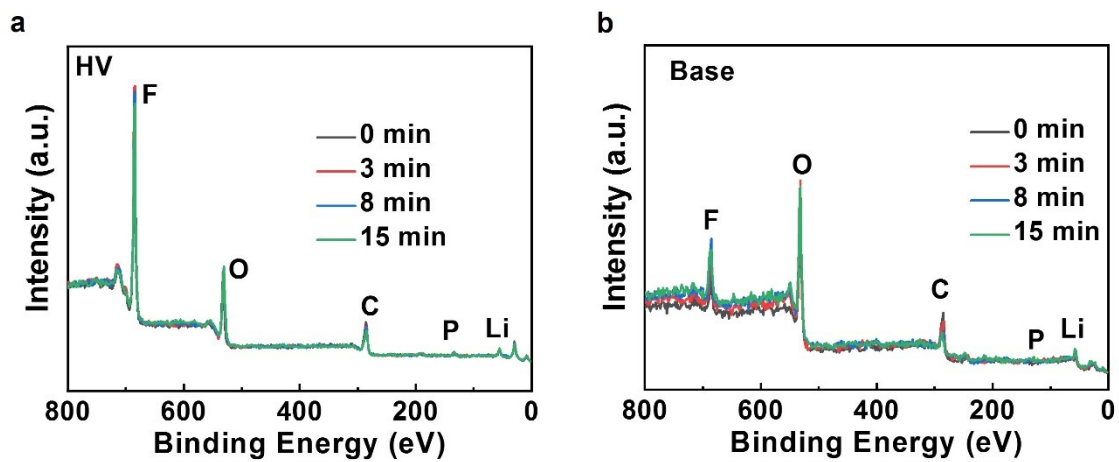


**Figure S6.** XPS spectra of the SEI formed in (a) HV and (b) base electrolytes.

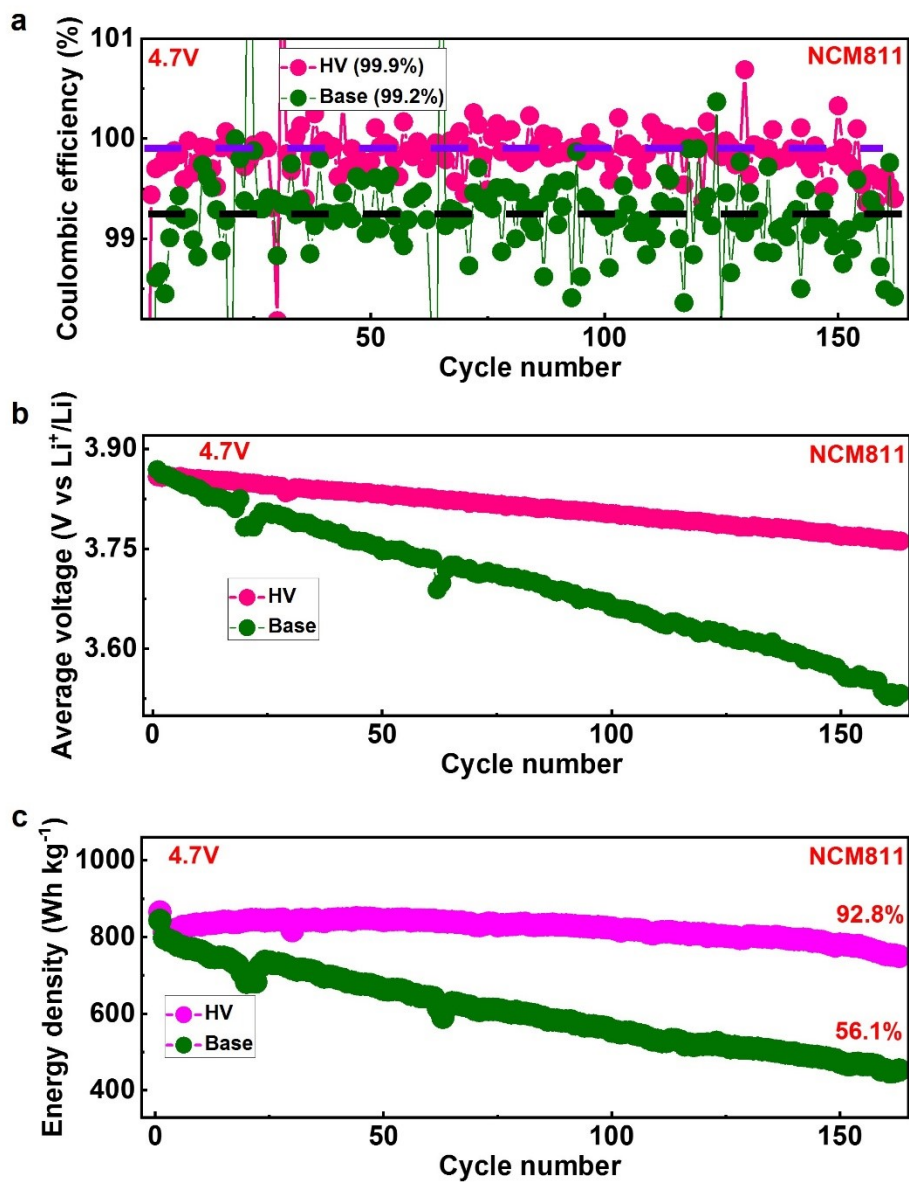


**Figure S7.** (a) Coulombic efficiency, (b) average voltage, and (c) energy density of Li||NCM811 cells using the different electrolytes at 0.5 C with a cut-off voltage of 4.7 V

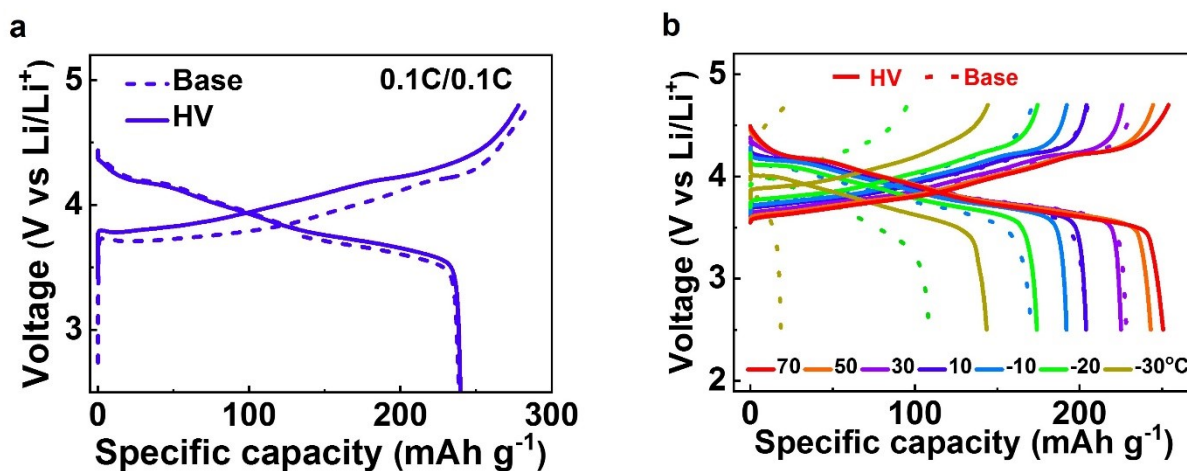


**Figure S8.** (a) Charge-discharge curves of Li||NCM811 cells using different electrolytes for the first cycle at 30 °C. (b) Charge-discharge curves of Li||NCM811 cells using the different electrolytes at different temperatures.

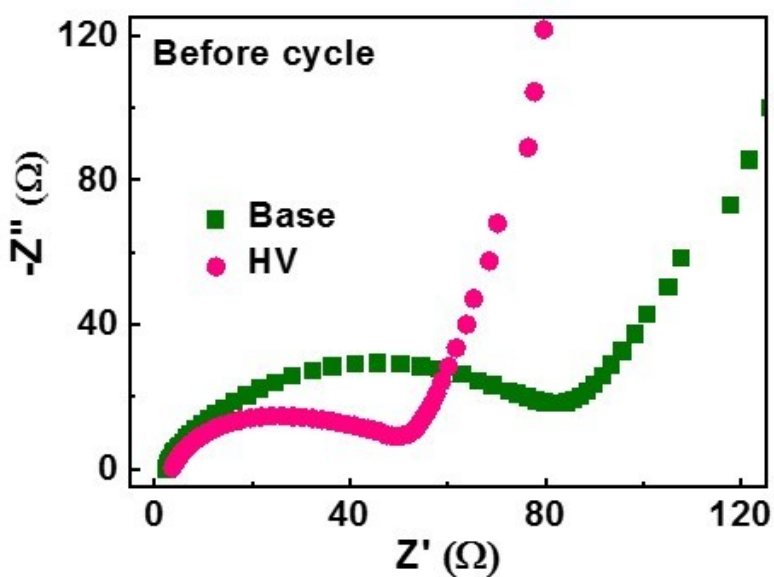


**Figure S9.** Nyquist plots of EIS tests of Li||NCM811 cells at room temperature.



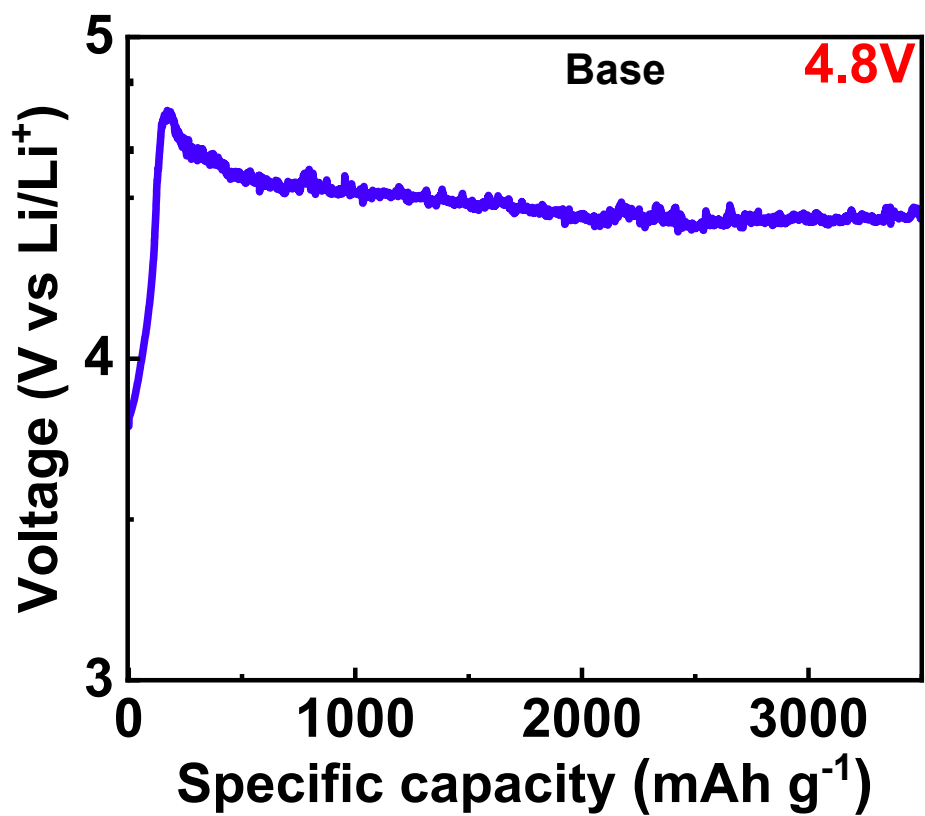


**Figure S10.** Charge curve of Li||NCM811 full cells using the base electrolyte.

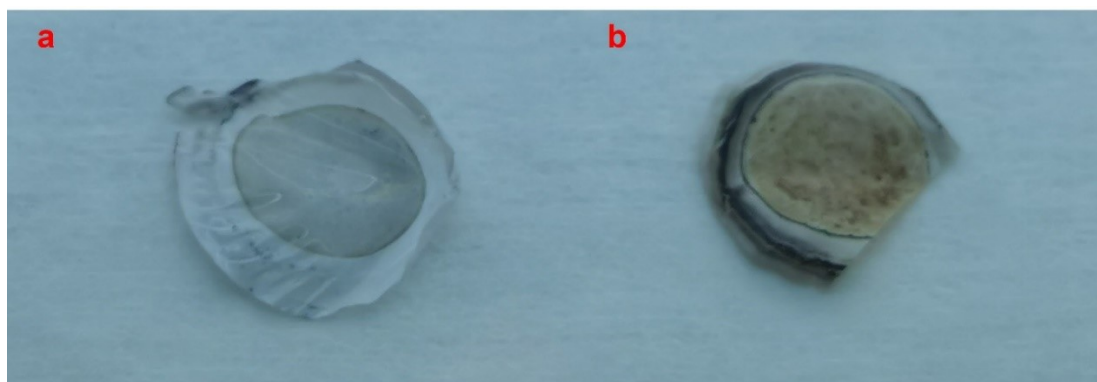


**Figure S11.** Separators of the Li||NCM811 cells using (a) HV and (b) base electrolytes after cycling at 55 °C.

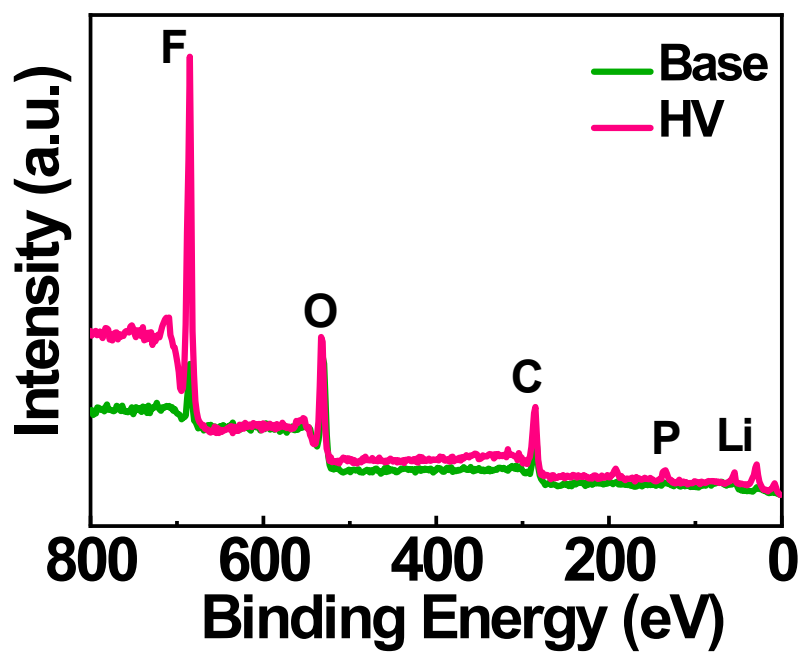


**Figure S12.** XPS spectra of the SEI formed in Li||NCM811 cells after cycling at 55 °C using the different electrolytes.

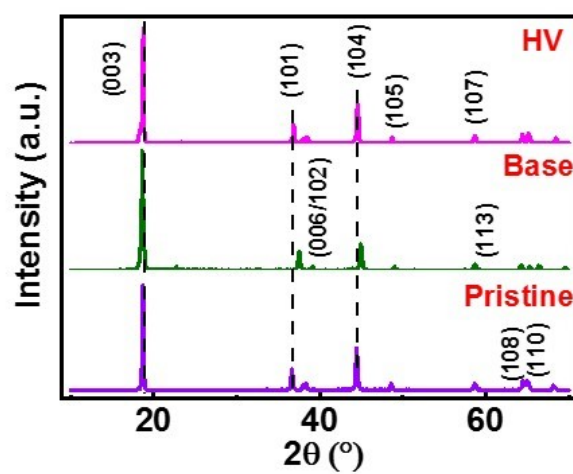


**Figure S13.** XRD spectra of pristine and NCM811 cycled in the different electrolytes.

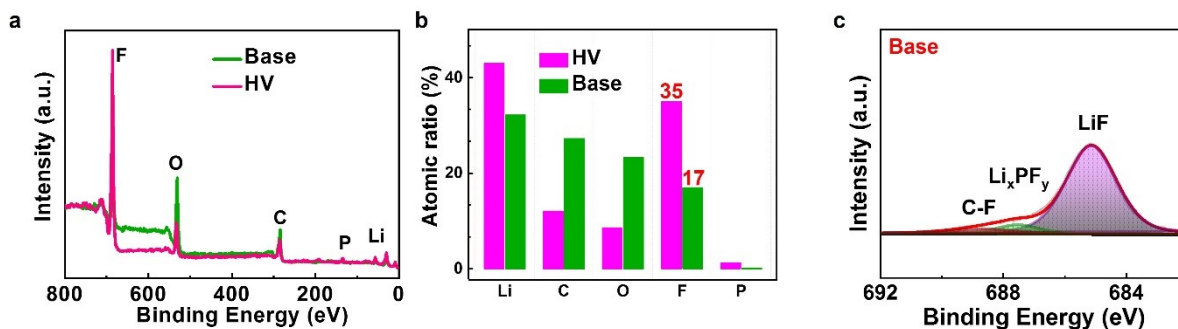


**Figure S14.** (a) XPS spectra of CEI formed in Li||NCM811 cells using the different electrolytes. (b) Atomic contents derived from the XPS spectra of the CEI formed on cycled NCM811 particles using the different electrolytes. (c) XPS spectra of F *1s* of CEI using the base electrolyte.

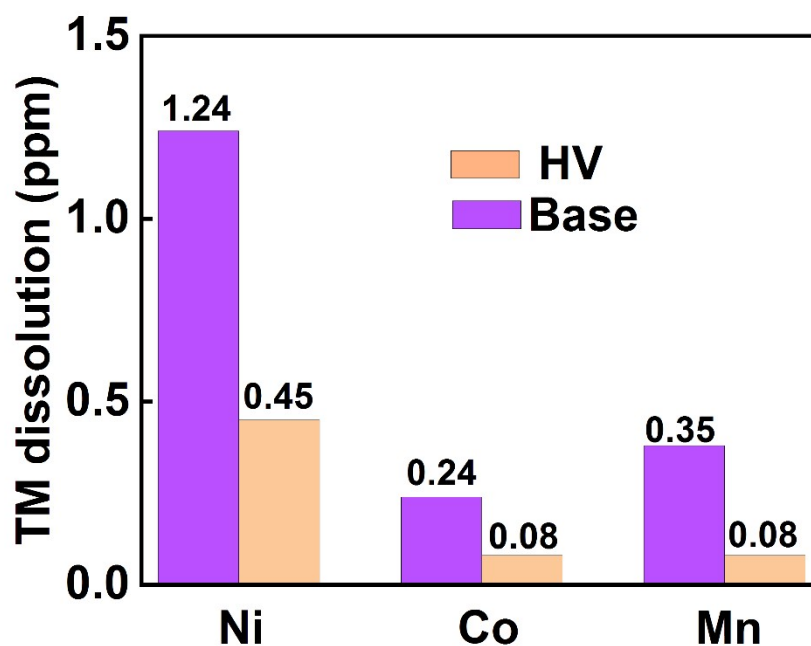


**Figure S15.** Transition metal ions (TM) dissolution measured by ICP-MS after cycling in different electrolytes